Static and dynamic properties of coupled electron-electron and electron-hole layers

Lerwen Liu and L. Świerkowski
School of Physics, The University of New South Wales, Sydney 2052, Australia

D. Neilson
School of Physics, The University of New South Wales, Sydney 2052, Australia and Scuola Normale Superiore, Piazza dei Cavalieri 7, 56126 Pisa, Italy

J. Szymański
Telecom Australia Research Laboratories, 770 Blackburn Road, Clayton 3168, Australia

(Received 12 October 1994; revised manuscript received 2 November 1995)

We have investigated coupled layers of electron and hole liquids in semiconductor heterostructures in zero magnetic field for densities $r_s \lesssim 20$ using the Singwi-Tosi-Land-Sjölander self-consistent formalism generalized for layers of unequal density. We calculate susceptibilities, local fields, pair correlation functions, and the dispersion of the collective modes for a range of layer spacings. We include cases where the densities in the two layers are not equal. We find generally that static correlations acting between layers do not have a large effect on the correlations within the layers. For coupled electron-hole layers we find that as the spacing between the layers decreases there is a divergence in the static susceptibility of the liquid that signals an instability towards a charge-density-wave ground state. When the layer spacing approaches the effective Bohr radius the electron-hole correlation function starts to diverge at small interparticle separations. This effect is a precursor to the onset of excitonic bound states but this is preempted by the charge-density-wave instability. The acoustic plasmon exhibits a crossover in behavior from a coupled mode to a mode that is confined to a single layer. Correlations sometimes push the acoustic plasmon dispersion curve completely into the single-particle excitation spectrum. For layers with different densities the Landau damping within the single-particle excitation region is sometimes so weak that the acoustic plasmon can exist inside the region as a sharp resonance. We find for the electron-hole case that proximity to the charge-density-wave instability has an unusual effect on the dispersion of the optical plasmon mode.

I. INTRODUCTION

There has been considerable recent interest in systems consisting of two parallel layers of electron or hole liquids trapped on adjacent quantum wells in a semiconductor heterostructure. The densities of the charge carriers in the two layers can be separately adjusted by using suitable gates on the top and bottom surfaces of the sample.[1] The presence of mobile charge in a second layer makes the behavior of the system distinctively different from the behavior of a single isolated layer, the charges in one layer acting as a polarizable background for charges in the other layer. The correlations between charges within the same layer, the intralayer correlations, and correlations between charges in opposite layers, the interlayer correlations, are quite different in nature.

In this paper we investigate static and dynamic properties of two-layer systems when there is no tunneling between the layers and no magnetic field. We self-consistently include the effect of correlations both within each layer and between the layers using the STLS approach developed by Singwi, Tosi, Land, and Sjölander[2] generalized for a two-component system.[3] In the STLS approach the effect of correlations is represented by local fields that modify the effective interaction between the charges. The local fields are determined self-consistently. Unlike previous work we do not restrict ourselves to the case where the densities in each layer are the same and we find when the layers are of unequal density that Landau damping of the collective modes inside the single-particle excitation region can be remarkably small.

There have been many theoretical studies of the two-layer system where correlations have been neglected. The collective modes were determined within the random phase approximation (RPA) by Das Sarma and Madhukar[4,5] and by Santoro and Giuliani.[6] Jain and Das Sarma[7] carried out an exhaustive RPA calculation for the collective mode dispersion including the effects of finite layer width and intersubband transitions.

The collective modes for nonidentical layers were studied by Eguiluz *et al.*[8] They found for a double inversion layer with electrons and holes of different effective mass that the dispersion curve of the heavier species (the holes) was significantly depressed while the curve for the lighter species (the electrons) was practically the same as the curve for a single layer. Das Sarma and Madhukar[5] subsequently identified these two modes with the optical and acoustic plasmons. Tzoar and Zhang[9] found if the effective masses of the carriers in the two layers were very different that the Landau damping of the acoustic plasmon within the single-particle excitation region can be very weak. There have been other studies of the Landau damping of the acoustic plasmon in related systems. Takada[10] studied this in multisubband systems, and Fasol *et al.*[11,12] found experimentally that in multiple-layer systems the Landau damping of collective modes by single-particle excitations can be weak. Finally, Platzman and Wolff[13] and Abstreiter, Cardona, and Pinczuk[14] have discussed this for three-dimensional systems and have pointed out that Laudau damping effects can be small in the excitation region between the two thresholds.

The effect of correlations in these systems has also been studied. Świerkowski, Szymański, and Gortel[15] have directly demonstrated the dramatic importance of correlations for electron-hole layers. Using STLS they showed that order of magnitude discrepancies in these systems between experimental transport measurements and the theoretical predictions of RPA could be quantitatively accounted for only by including correlations.

As an extreme case of strong interlayer correlations Lozovik and Yudson[16] and Shevchenko[17] considered dielectric pairing of the spatially separated electrons and holes. They proposed when the effective pairing interaction was sufficiently strong that the system could make a transition to the superfluid state of an exciton gas. When the spacing between the layers exceeded the effective Bohr radius $a_B^\star$ the correlations were much weaker and the probability of exciton formation was found to decrease exponentially with layer spacing.

Tselis and Quinn[18] treated correlations for two electron layers using a self-consistent-field approach that includes resonant screening and vertex corrections while Kalman and Golden[19] used a quasilocalized charge approximation. Świerkowski, Neilson, and Szymański[20] took into account correlations within each layer using a static local field that was deduced from numerical simulation data for a single layer[21] but they neglected correlations between the layers. They demonstrated that the correlations could generate ground states that are spatially inhomogeneous in the electron density parallel to the layers. Using the same approach dynamic properties of this system at low densities were investigated by Neilson *et al.*[22] Szymański and co-workers[23] subsequently calculated the interlayer correlations using STLS while keeping the correlations within the layers fixed at the values determined in Ref. 21 for a single layer. They found that inclusion of interlayer correlations tended to suppress the instability towards inhomogeneous ground states for two layers of electrons but it had little effect on the instability for electron-hole layers.

Gold[24] used the STLS approach in a related system consisting of a superlattice of parallel electron layers to show quite generally that many-body correlations generate an inhomogeneous ground-state instability corresponding to a charge density wave. For the two-layer system Gold used STLS but he approximated the local field correction within the layers by the small wave number STLS local field for a single layer and he neglected the local fields corresponding to correlations between the layers altogether. Zhang[25] carried out a full STLS calculation to determine both the intralayer and interlayer local fields self-consistently and from this he determined the static structure factors. We have repeated this calculation and obtain significantly different results for both the local fields and the structure factors. Zhang also analytically determined a critical spacing below which the low-lying acoustic plasmon will be strongly Landau damped. Zheng and MacDonald[26] used the STLS to calculate static

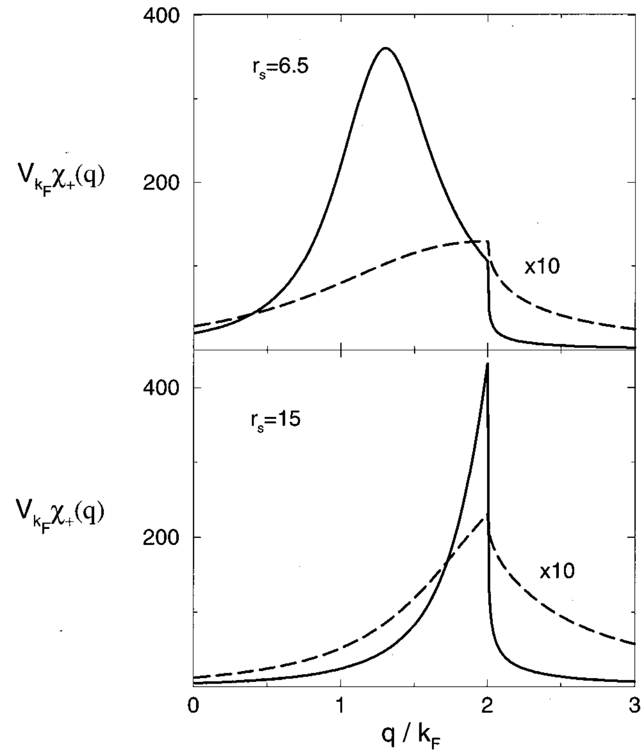

FIG. 1. Static susceptibility $\chi_+(\boldsymbol{q})$ for the in-phase normal mode for electron-hole layers. Dashed lines are for layer spacings of $d=2d_i$ and solid lines for $d=1.05d_i$ where d_i is the spacing at which $\chi_+(\boldsymbol{q})$ diverges. The $d=2d_i$ curves have been multiplied by a factor of 10.

properties of the two-layer system. They determined the correlation energy, the intralayer and interlayer pair distribution functions and the electron momentum distribution. All these calculations considered only layers of equal density.

In Ref. 23 the correlations between layers and within the layers were determined using different approximations. Here we use the STLS approach to calculate both sets of correlations self-consistently with the same level of approximation. This approach cannot be used at extremely low densities where correlations within the layers are too strong. The present work thus complements the approach in Ref. 23, which can be applied all the way down to Wigner crystallization densities but only when the layers are sufficiently far apart for the correlations between the layers not to have grown too strong.

In this paper we report on new results for static and dynamic properties of two-layer systems. In Sec. II we outline the STLS formalism that we have generalized for layers of unequal density. Section III discusses the charge density instability and the new soft-mode in the low-lying collective excited-state spectrum. Section IV presents the static local fields and pair correlation functions and discusses their dependence on the distance between the layers. Section V describes properties of the collective modes in the system both when the layers are of equal density and also when the densities are different. The collective mode properties are not restricted to the region of small wave numbers and the effect of the Landau damping of the plasmons is reexamined. Section VI contains concluding remarks.

II. THEORY

The system we consider consists of two parallel layers, one containing electrons and the other either electrons or holes. Motion in the z direction is confined to the layers by two quantum wells separated by a distance d. We consider only zero temperature and zero magnetic field.

The total response function matrix $\chi_{\ell\ell'}(\boldsymbol{q},\omega)$ of the two-layer system[20] when diagonalized has elements,

$$\chi_{\pm}(\boldsymbol{q},\omega)=\frac{2}{\chi_1^{-1}(\boldsymbol{q},\omega)+\chi_2^{-1}(\boldsymbol{q},\omega)\pm\eta_{12}\sqrt{\{\chi_1^{-1}(\boldsymbol{q},\omega)-\chi_2^{-1}(\boldsymbol{q},\omega)\}^2+4\{[1-G_{12}(\boldsymbol{q})]V_{12}(\boldsymbol{q})\}^2}}, \tag{1}$$

where $V_{\ell\ell'}(\boldsymbol{q})=\eta_{\ell\ell'}V_{\boldsymbol{q}}\exp(-q|\ell-\ell'|d)$, with $V_{\boldsymbol{q}}=(2\pi e^2)/|\boldsymbol{q}|$, is the Coulomb interaction between carriers in layers ℓ and ℓ' and the $G_{\ell\ell'}(\boldsymbol{q})$ are the corresponding static local fields that modify these bare interactions. $\eta_{\ell\ell'}=1$ for electron-electron layers and $(-1)^{|\ell-\ell'|}$ for electron-hole layers. $\chi_{\ell}(\boldsymbol{q},\omega)$ is the response function of a single isolated layer ℓ, which we take to be

$$\chi_{\ell}(\boldsymbol{q},\omega)=\frac{\chi_{\ell}^{(0)}(\boldsymbol{q},\omega)}{1+V_{\ell\ell}(\boldsymbol{q})[1-G_{\ell\ell}(\boldsymbol{q})]\chi_{\ell}^{(0)}(\boldsymbol{q},\omega)}, \tag{2}$$

where $\chi_{\ell}^{(0)}(\boldsymbol{q},\omega)$ is the Lindhard function of the two-dimensional electron or hole system.[27]

Within the STLS approach[2] for the two-component system[3] the local fields are related to the static structure factors $S_{\ell\ell'}(\boldsymbol{q})$ through the expression[23]

$$G_{\ell\ell'}(\boldsymbol{q})=-\frac{1}{\sqrt{n_{\ell}n_{\ell'}}}\int\frac{d^2\boldsymbol{k}}{(2\pi)^2}\frac{(\boldsymbol{q}\cdot\boldsymbol{k})}{q^2}\frac{V_{\ell\ell'}(\boldsymbol{k})}{V_{\ell\ell'}(\boldsymbol{q})}\times[S_{\ell\ell'}(|\boldsymbol{q}-\boldsymbol{k}|)-\delta_{\ell\ell'}], \tag{3}$$

where n_{ℓ} is the mean density in layer ℓ. The static structure factors are related to the response functions by the exact fluctuation-dissipation theorem. Equations (1) and (3) form a closed set of equations that can be solved self-consistently for the local fields $G_{\ell\ell'}(\boldsymbol{q})$.

The pair correlation functions $g_{\ell\ell'}(\boldsymbol{r})$ that give the probability that two charges in layers ℓ and ℓ' are separated by a distance $|\boldsymbol{r}|$ parallel to the layers can be obtained in the usual way from the Fourier transform of $[S_{\ell\ell'}(\boldsymbol{q})-\delta_{\ell\ell'}]$.[23]

III. CHARGE-DENSITY-WAVE INSTABILITY

To detect a charge-density-wave instability in the ground state we look for a divergence in $\chi_{\pm}(\boldsymbol{q})$, the static response of the normal modes to an external stimulus of wave number $|\boldsymbol{q}|$. A divergence is caused by the denominator in Eq. (1) vanishing for zero ω. This may occur depending on the magnitudes of the local fields $G_{\ell\ell'}(q)$.

For electron-hole layers we find that the liquid ground state does become unstable as the spacing between the layers is reduced. In Fig. 1 the dashed lines show $\chi_{+}(\boldsymbol{q})$ for a layer spacing well away from the instability. $\chi_{+}(\boldsymbol{q})$ is not large and for clarity these lines have been multiplied by a factor of 10. The solid lines are $\chi_{+}(\boldsymbol{q})$ for a spacing close to the value d_i at which the instability occurs. Very near the instability it becomes difficult to obtain convergent solutions and to determine the d_i for the actual instability we extrapolate the values of $1/\chi_{+}(\boldsymbol{q})$ to zero for a set of decreasing interlayer spacings. The density parameter $r_s=(\sqrt{\pi n}a_B^{\star})^{-1}$, where n is the mean density in one layer. For $r_s=6.5$ the $\chi_{+}(\boldsymbol{q})$ diverges at a spacing of $d_i=1.9a_B^{\star}$. In gallium arsenide $a_B^{\star}=9.8$ nm so this is $d=18.6$ nm. $\chi_{+}(\boldsymbol{q})$ diverges for a $|\boldsymbol{q}|/k_F$ value of 1.3, where k_F is the Fermi momentum within a layer. For $r_s=15$ the divergence occurs for a spacing of $d_i=7.2a_B^{\star}$ at $|\boldsymbol{q}|/k_F\simeq 2$.

The fact that the divergence occurs at nonzero values of $|\boldsymbol{q}|$ is indicative of a second-order phase transition to a ground state that is inhomogeneous in the density with periodic wave number of $|\boldsymbol{q}|$. We cannot draw any definite conclusion since a first-order transition at a layer spacing $d>d_i$ could preempt this and is not detectable by the formalism. If the transition is in fact second order then the inhomogeneous ground state is probably a charge density wave.

We recall in a previous calculation we obtained a similar instability in this system.[23] The correlations were determined there differently, the interlayer correlations being calculated using STLS while correlations within each layer were deduced from numerical simulation data for the single layer case.[21]

The instability is accompanied by the development of a

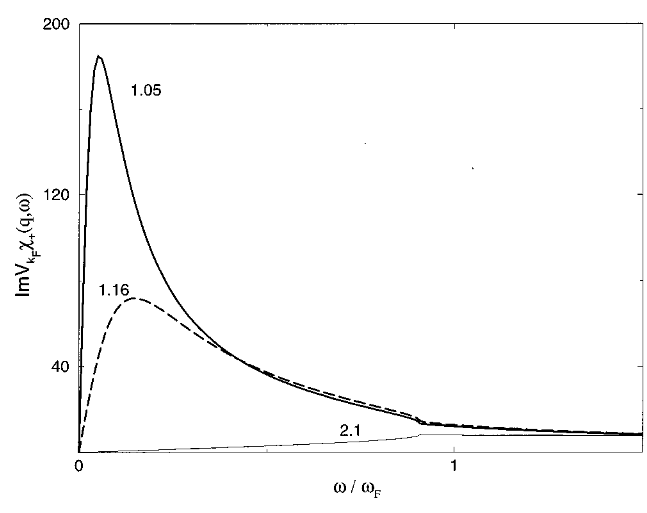

FIG. 2. Dynamic structure factor $\mathrm{Im}\chi_{+}(\boldsymbol{q},\omega)$ for fixed $|\boldsymbol{q}|/k_F=1.3$ for electron-hole layers at $r_s=6.5$. The curves are for different layer spacings in units of d_i. $\hbar\omega_F$ is the Fermi energy.

soft mode at finite $|\boldsymbol{q}|$. This is seen in Fig. 2, which shows $\mathrm{Im}\chi_+(\boldsymbol{q},\omega)$ at $r_s=6.5$ for fixed $|\boldsymbol{q}|/k_F=1.3$. As the layer spacing is decreased a sharp peak develops at small ω so that it costs very little energy to excite an inhomogeneous state with wave numbers $|\boldsymbol{q}|/k_F\simeq 1.3$. Decreasing the spacing makes the peak grow higher and move towards zero ω so that spontaneous fluctuations into the inhomogeneous excited state can remain for increasingly long periods of time and the liquid starts to become unstable. As the layer spacing approaches d_i the position of the peak in $\mathrm{Im}\chi_+(\boldsymbol{q},\omega)$ goes to $\omega=0$. This is characteristic behavior of a soft mode. Experimental observation of the soft mode in the form of a new peak appearing in the imaginary part of the liquid dielectric response function at small ω and finite $\boldsymbol{q}$ would indirectly confirm the appearance of an inhomogeneous ground state.

For two coupled layers of electrons we find no divergence in $\chi_\pm(\boldsymbol{q})$. This important difference between electron-hole layer and electron-electron layer systems may be understood as follows. Formation of an inhomogeneous ground state depends on the result of a competition between the potential energy gain from matching inhomogeneous density distributions in the two layers[20] and the increased amount of screening from the proximity of the mobile charges in the two layers. An increase in screening reduces the strength of the correlations in the system and thus favors the homogeneous liquid state. If we compare the electron-hole and electron-electron layer systems a key difference is that the additional potential energy gain favoring the inhomogeneous state is much greater for electron-hole layers with their attractive interactions than it is for the repulsive interactions between a pair of electron layers.

IV. STATIC PROPERTIES

A. Local fields

In Fig. 3(a) we show the local fields for two electron layers each at density $r_s=4$ and also the local field $G(\boldsymbol{q})$ obtained from an STLS calculation for a single $r_s=4$ layer. It is interesting to note as the layers are brought closer together that the interlayer local field $G_{12}(\boldsymbol{q})$ is strongly affected but the intralayer field $G_{11}(\boldsymbol{q})$ is much less sensitive. In fact for $d>20$ nm the form of $G_{11}(\boldsymbol{q})$ is not significantly different from the single layer $G(\boldsymbol{q})$ so correlations within a layer are not affected by the proximity of a second layer. In

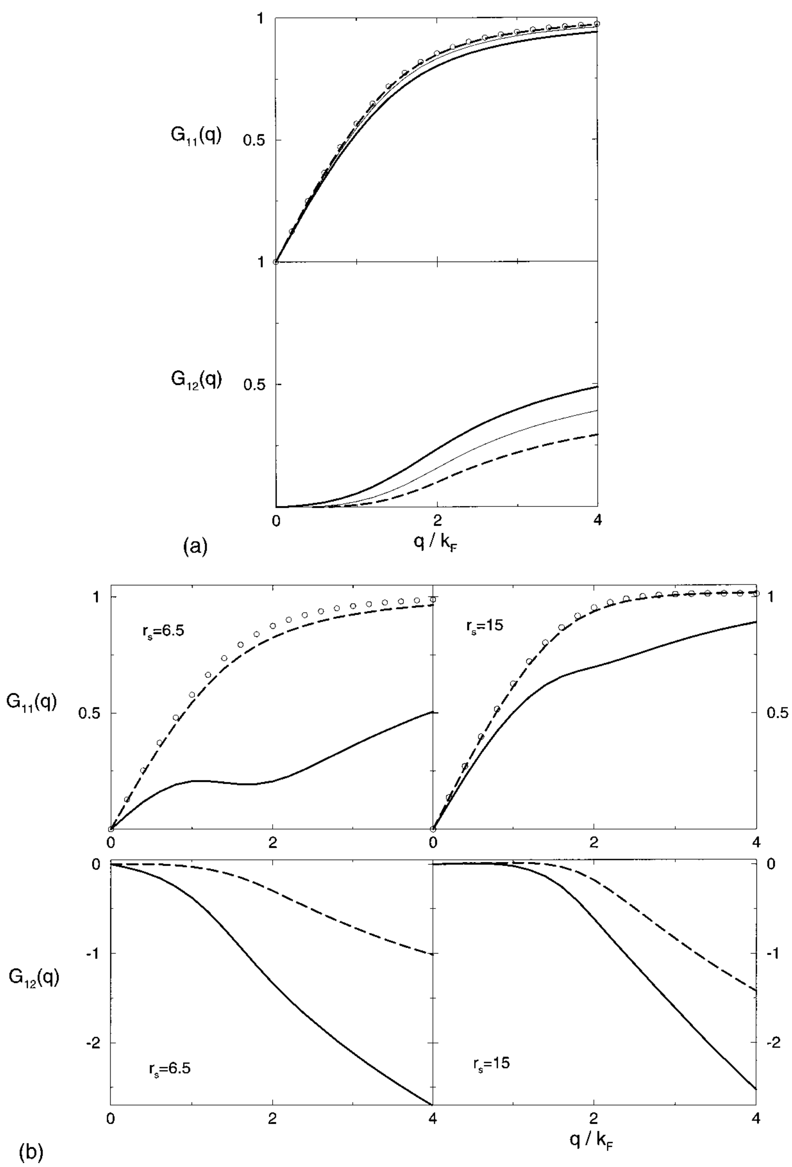

FIG. 3. (a) Local fields $G_{11}(\boldsymbol{q})$ and $G_{12}(\boldsymbol{q})$ for two electron layers each of density $r_s=4$. Layer spacings are $d=20$ nm (thick solid lines), $d=30$ nm (thin solid lines), and $d=50$ nm (dashed lines). Circles show the local field $G(\boldsymbol{q})$ for a single $r_s=4$ layer. (b) Local fields $G_{11}(\boldsymbol{q})$ and $G_{12}(\boldsymbol{q})$ for electron-hole layers. Layer spacings are $2d_i$ (dashed lines) and $1.05d_i$ (solid lines). Circles are the local field $G(\boldsymbol{q})$ for a single layer at the same density.

contrast the interlayer local field $G_{12}(\boldsymbol{q})$ is sensitive to the spacing between layers even for $d \gtrsim 50$ nm. This steady increase in $G_{12}(\boldsymbol{q})$ for $q/k_F \gtrsim 1$ reflects the buildup in the interlayer correlations.

Zhang[25] has previously calculated the local fields and static structure factors for two electron layers using the STLS formalism. The structure factors we obtain are smooth and do not show any of the cusplike behavior near $|\boldsymbol{q}|/(2k_F) \simeq 0.6$ discussed in Ref. 25. If we compare our results for the local fields with those in Fig. 2(b) of Ref. 25 for density $r_s = 2\sqrt{2}$ (there is a $\sqrt{2}$ difference in our definitions of r_s) then we find for all $\boldsymbol{q}$ that our $G_{11}(\boldsymbol{q})$ is approximately twice that of the $G_{11}(\boldsymbol{q})$ in Ref. 25. Also the linear gradient of our $G_{12}(\boldsymbol{q})$ at small $\boldsymbol{q}$ is much smaller than the linear gradient of the $G_{12}(\boldsymbol{q})$ in Ref. 25. Due to some misprints in Ref. 25 it is not possible to identify the precise source of the error there.

Figure 3(b) shows the local fields $G_{11}(\boldsymbol{q})$ and $G_{12}(\boldsymbol{q})$ for electron-hole layers. In one case the layer spacing is well away from the instability $d \gg d_i$ and in the other it is close to d_i. The STLS local field $G(\boldsymbol{q})$ for a single layer at the same density is again shown. Note that for small $\boldsymbol{q}$ the local fields always exhibit linear behavior. The interlayer local field $G_{12}(\boldsymbol{q})$ is negative because of the attractive electron-hole interaction. Its magnitude becomes steadily larger for decreasing spacing. This indicates a continuous increase in the strength of the attractive correlations between the electrons and holes. As in the electron-electron case $G_{11}(\boldsymbol{q})$ approximates the single layer $G(\boldsymbol{q})$ at larger layer spacings but as d approaches d_i the $G_{11}(\boldsymbol{q})$ becomes less than $G(\boldsymbol{q})$. This indicates that near the instability correlations within the planes become weaker.

In comparing the local fields for electron-hole and electron-electron layers we see apart from the obvious change in the sign of $G_{12}(\boldsymbol{q})$ in going from one system to the other less expected property. This is the much stronger cross dependence we have noted between $G_{11}(\boldsymbol{q})$ and $G_{12}(\boldsymbol{q})$ in the electron-hole system compared with two electron layers. This is particularly evident near the instability.

B. Pair correlation functions

In Fig. 4(a) we compare the pair correlation functions for two electron layers of density $r_s = 4$ for different layer spacings and we also show the STLS pair correlation function $g(\boldsymbol{r})$ for a single $r_s = 4$ layer. For $d = 50$ nm $g_{12}(\boldsymbol{r})$ is everywhere close to unity so the interlayer correlations are weak. For $d = 30$ nm there is a dip in $g_{12}(\boldsymbol{r})$ around the origin, indicating the interlayer correlations are becoming important. By $d = 20$ nm the value of $g_{12}(\boldsymbol{r})$ at $\boldsymbol{r} = 0$ has dropped to 0.6. Since there is no exchange between layers this corresponds to strong interlayer correlations. However, this buildup has little effect on the correlations acting within a layer and even for $d = 20$ nm $g_{11}(\boldsymbol{r})$ remains close to $g(\boldsymbol{r})$. To the extent that there is some interdependence the trend is that as the correlations between layers become stronger the correlations within a layer get slightly weaker. This compensatory effect results from the increased screening of electron interactions in a layer by electrons from the second layer.[23]

In Fig. 4(b) the dependence of the pair correlation functions on the spacing between electron-hole layers is shown. The intralayer correlation function $g_{11}(\boldsymbol{r})$ approximates the single-layer correlation function $g(\boldsymbol{r})$ for layer spacings $d \gtrsim 2d_i$ but when we decrease the spacing to approach the instability $d \simeq d_i$ the $g_{11}(\boldsymbol{r})$ develops a new peak around $|\boldsymbol{r}|k_F \simeq 1$ and oscillates for larger $\boldsymbol{r}$. These effects are indications of the proximity of an inhomogeneous ground state.

In contrast to this, over the same range of spacings the correlation function $g_{12}(\boldsymbol{r})$ shows a steady buildup in the electron-hole correlations. Even for $d = 2d_i$ there is a significant buildup of correlations in $g_{12}(\boldsymbol{r})$ at small $\boldsymbol{r}$. This buildup is probably a precursor to the formation of exciton bound states[28] between electrons and holes from the different layers and is not directly related to the charge-density-wave instability.

In our calculation the onset of the instability in the liquid occurs before exciton states could form but we can estimate the layer spacing at which they would have formed by extrapolating $1/g_{12}(\boldsymbol{r})|_{\boldsymbol{r}=0}$ as a function of d to locate where it would go to zero. Figure 5 gives a value $d \simeq 1.2a_B^\star$ for $r_s = 6.5$ while at $r_s = 15$ the value is $d \approx 2a_B^\star$. This would indicate that excitonic formation becomes easier at lower densities where the screening of the electron-hole interactions is weaker. Our results suggest that excitons can form when the electron and holes are kept at distances greater than the Bohr radius. This is consistent with Lozovik and Yudson's[16] result that excitons can exist for layer spacings greater than $a_B^\star$ but with significantly smaller binding energies than free excitons.

V. PLASMONS

There are two plasmon collective modes in these systems.[5] At small $\boldsymbol{q}$ the higher-energy mode, the optical branch, approaches zero as $\hbar\omega \sim \sqrt{|\mathbf{q}|}$, which is the same behavior as a plasmon in a single layer. For the lower-lying mode the energy vanishes linearly with $\boldsymbol{q}$, an acousticlike behavior caused by screening of the long-range part of the Coulomb potential by charges in the opposite layer.

A. Critical spacing

Correlations usually have little effect on the small $\boldsymbol{q}$ dispersion of a plasmon since correlations are weak when electrons are far apart. However, for these systems the acoustic branch is sensitive to correlations even for very small $\boldsymbol{q}$. The correlations can sometimes reduce the gradient of the acoustic plasmon dispersion curve so much that the curve merges completely with the single-particle excitation spectrum.

We can determine the critical layer spacing d_c, below which the acoustic plasmon lies totally within the single-particle excitation region, by applying the power expansion method used in Ref. 6. The critical spacing occurs when the small $\boldsymbol{q}$ gradient of the acoustic plasmon curve equals the gradient of the single-particle excitation region. The general expression for the critical spacing is given by

$$d_c = \left[\frac{G'_{11} + G'_{22} - 2G'_{12}}{2}\right] + \left[\frac{a^\star_{B_1}}{4}\frac{\sqrt{1-(v_{F_1}/v_{F_2})^2}}{[1-\sqrt{1-(v_{F_1}/v_{F_2})^2}]}\right], \tag{4}$$

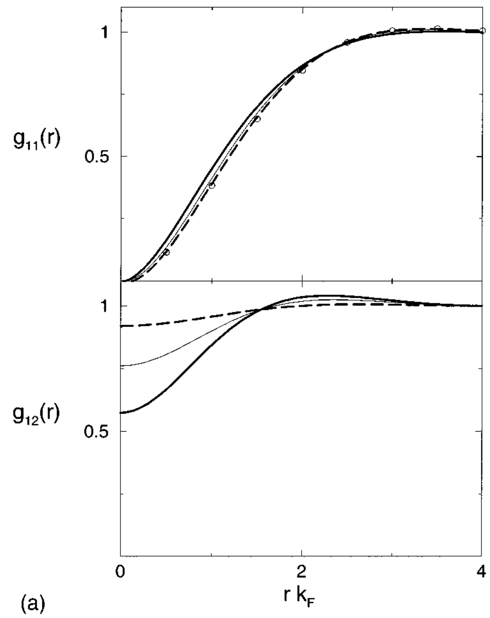

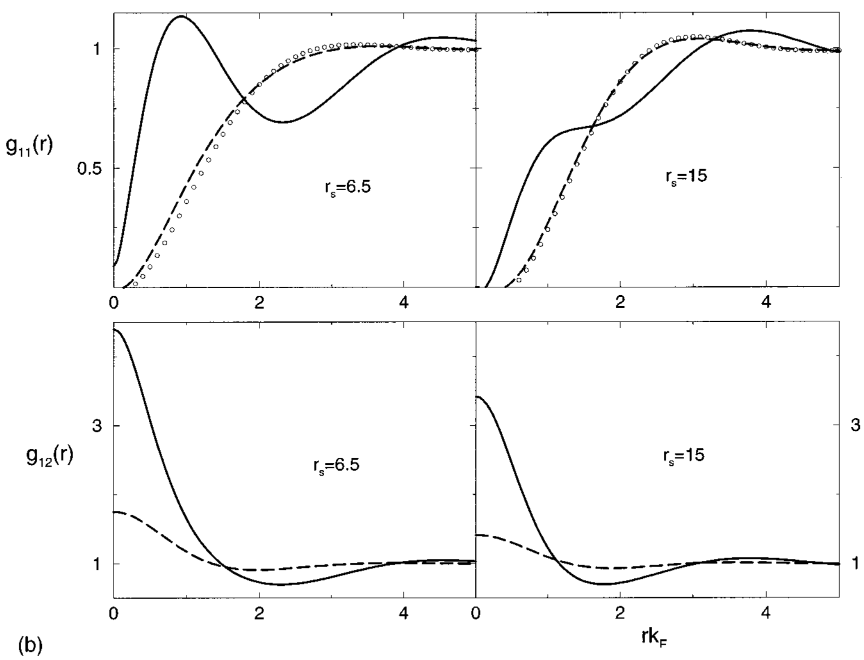

FIG. 4. (a) Pair correlation functions $g_{11}(\boldsymbol{r})$ and $g_{12}(\boldsymbol{r})$ for two electron layers of density $r_s=4$. Layer spacing is $d=20$ nm (thick solid lines), $d=30$ nm (thin solid lines), and $d=50$ nm (dashed lines). Circles show $g(\boldsymbol{r})$ for a single $r_s=4$ layer. (b) In-plane and interplane pair correlation functions $g_{11}(\boldsymbol{r})$ and $g_{12}(\boldsymbol{r})$ for electron-hole layers. Layer spacings are $2d_i$ (dashed lines) and $1.05d_i$ (solid lines). Circles are the pair correlation function $g(\boldsymbol{r})$ for a single layer at the same density.

where we have taken layer 1 to have the smaller Fermi velocity, $v_{F_1} \leqslant v_{F_2}$, and $a^{\star}_{B_1}$ is the effective Bohr radius of layer 1. The $G'_{\ell\ell'}$ are the small-$\boldsymbol{q}$ limiting gradients of the local fields, $G'_{\ell\ell'} \equiv \lim_{\boldsymbol{q}\to 0}[dG_{\ell\ell'}(\boldsymbol{q})/d|\boldsymbol{q}|]$.

For identical layers Eq. (4) within the RPA gives $d_c=0$, implying for all spacings that the RPA acoustic plasmon exists outside the single-particle excitation region for small $\boldsymbol{q}$.[6] For identical layers with correlations the critical spacing is $d_c=[G'_{11}-G'_{12}]$. From Fig. 3 we see that G'_{12} is negligibly small compared with G'_{11}, and since $G'_{11}>0$ local field effects must lead to $d_c>0$.

Reference 25 also gives an expression for the critical spacing between the layers in the case of identical layers but the expression is incorrect because the small-frequency Lindhard function is calculated using a limiting wave-number-to-frequency ratio of $|\boldsymbol{q}|/\omega=0$, which is not the correct one for a dispersion curve vanishing linearly with $|\boldsymbol{q}|$.[6]

Gold[24] also discusses the suppression of the plasmon mode by correlations but he uses an approximation where the plasmons are undamped for all momentum and energy transfers. Their energy approaches zero at the point of instability to the charge-density-wave ground state. Before this could happen, however, the plasmons would have already merged with the single-particle excitation spectrum and been damped out.

B. Electron-electron layers

Figure 6 shows the plasmon dispersion curves for two $r_s=4$ electron layers separated by $d=20$ nm. For wide spacings between the layers the dispersion curves of both plasmons at large values of $\boldsymbol{q}$ approach the curve for the single layer plasmon. This is because as $\boldsymbol{q}$ increases the Coulomb coupling between layers gets weaker. There is the same trend at smaller spacings but there the plasmons enter the single-particle excitation region before it can occur.

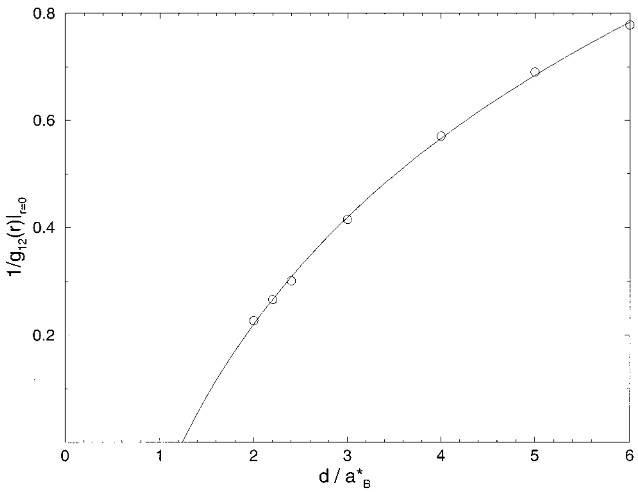

FIG. 5. Points show $1/g_{12}(\boldsymbol{r})|_{\boldsymbol{r}=0}$ as a function of the spacing between an electron and hole layer. The density is $r_s=6.5$. The line is an extrapolation indicating that $1/g_{12}(\boldsymbol{r})|_{\boldsymbol{r}=0}$ would vanish at $d=1.2a_B^\star$.

For two electron layers at $r_s=4$ the critical spacing at which the acoustic plasmon is totally absorbed into the single-particle excitation region is $d_c\approx16$ nm. In Fig. 6 the acoustic plasmon is already nearly absorbed into the single-particle excitation region and exists only for very small $\boldsymbol{q}$.

Figure 7(a) shows the dispersion of plasmons for different layer spacings for two layers of unequal electron density, $r_s=4$ and 2. Also shown are the curves of plasmons in single layers at $r_s=4$ or 2. For wider spacings the dispersion curve of the acoustic plasmon at large $\boldsymbol{q}$ tends towards that for the single $r_s=4$ layer while the curve for the optical plasmon approaches the $r_s=2$ single-layer plasmon. This again reflects the presence of the $\exp(-|\boldsymbol{q}|d)$ factor in the expression $V_{12}(\boldsymbol{q})$ for the coupling between the layers. As d is made larger the crossover from coupled collective modes into single-layer mode behavior occurs at decreasing values of $\boldsymbol{q}$.

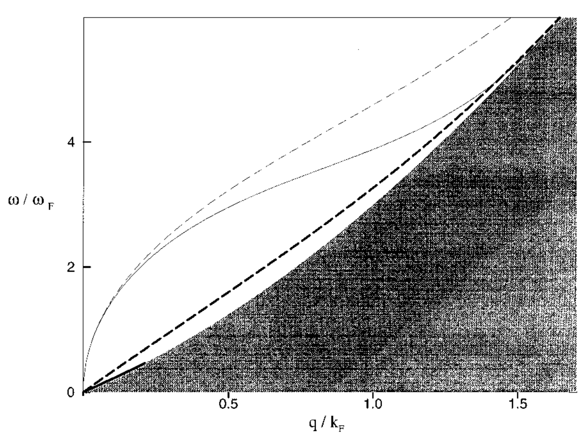

FIG. 6. Dispersion curves for the acoustic and optical plasmon branches for two $r_s=4$ electron layers (solid lines). Layer spacing is $d=20$ nm. Dashed lines are the RPA curves. Shaded area shows the single-particle excitation region for an $r_s=4$ layer.

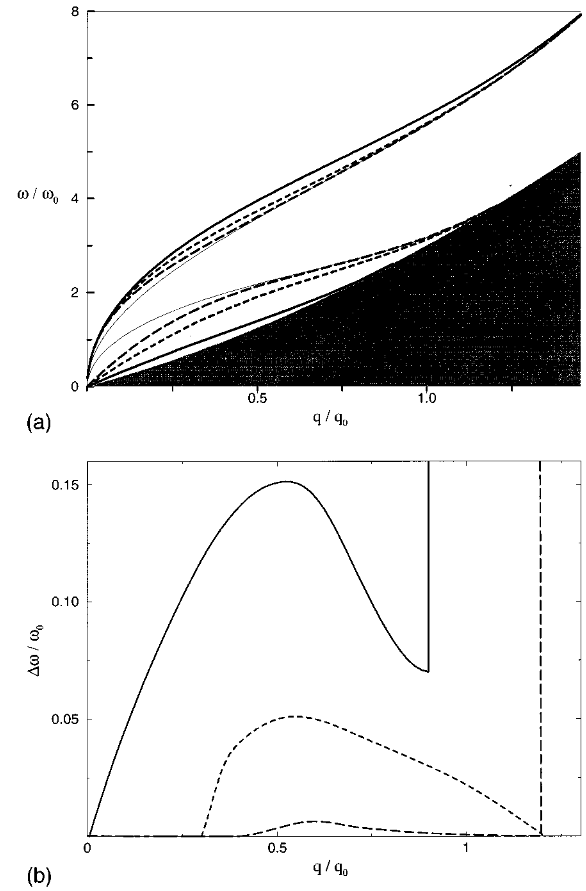

FIG. 7. (a) Thick lines are the dispersion curves for the acoustic and optical plasmon branches for two electron layers of unequal density, $r_s=4$ and 2. Layer spacings are $d=20$ nm (solid lines), $d=50$ nm (short-dashed lines), and $d=100$ nm (long-dashed lines). Upper thin line is the dispersion curve for a single layer at $r_s=2$ and lower thin line the curve for a single layer at $r_s=4$. Darker shaded area indicates the single-particle excitation region for an $r_s=4$ layer and lighter shaded area the excitation region for an $r_s=2$ layer. Constants $q_0=3.6\times10^5$ cm^{-1} and $\hbar\omega_0=0.61$ meV are the Fermi momentum and energy in the $r_s=4$ layer. (b) Relative widths of the acoustic plasmon for the same spacings as in (a). The sharp increase in width occurs at the $r_s=4$ single-particle excitation threshold.

We find when the two layers are not identical that the plasmon can continue to exist as a sharp resonance peak after it first enters the single-particle excitation region. Initially this region is associated with single-particle excitations from the layer of higher density. Landau damping does occur in this region but it is very small when the amplitude of the plasmon oscillations is concentrated principally in the layer of lower density. This phenomenon is illustrated in Fig. 7(b), which plots the width of the acoustic plasmon on the same horizontal axis as Fig. 7(a). When the plasmon reaches the first threshold q_{c_2} its width is determined by the imaginary part of $\chi_-(\boldsymbol{q},\omega)$ and in Fig. 7(b) we take the plasmon width to be the full width at half maximum of the peak in $\mathrm{Im}m\chi_-(\boldsymbol{q},\omega)$. Figure 7(b) shows that a sharp acoustic plasmon peak exists in the single-particle excitation region between the two thresholds $q_{c_2}\leqslant|\boldsymbol{q}|<q_{c_1}$. Only when the plasmon reaches the threshold for the lower density layer q_{c_1}

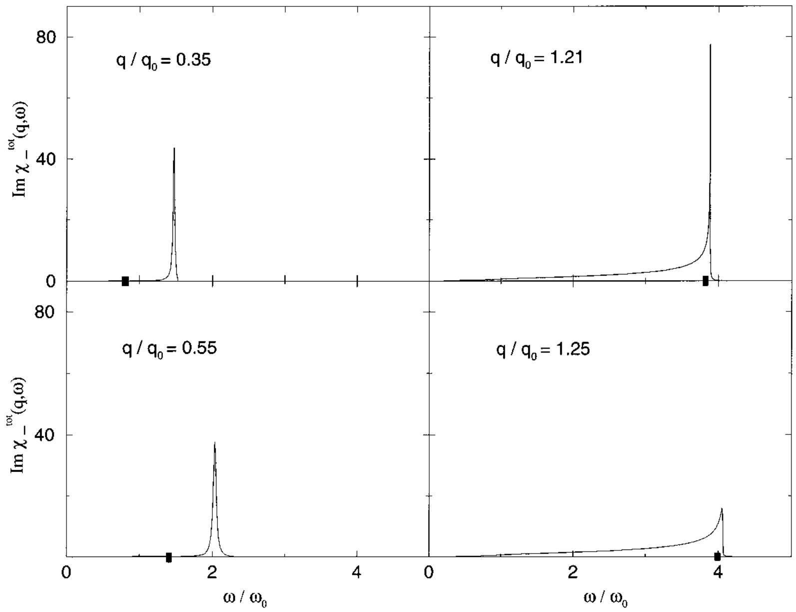

FIG. 8. Dynamic structure factor $\mathrm{Im}\chi_{-}(\boldsymbol{q},\omega)$ for two electron layers of unequal density, $r_s=4$ and 2. The layer spacing is $d=50$ nm. The values of $\boldsymbol{q}$ shown all lie within the $r_s=2$ single-particle excitation region. Constants q_0 and $\hbar\omega_0$ are the same as in Fig. 7. The mark on the ω axis indicates the single-particle threshold for the $r_s=4$ layer. For $0.30 \lesssim |\boldsymbol{q}|/q_0 \lesssim 1.22$ the acoustic plasmon is a sharp resonance lying inside the $r_s=2$ single-particle excitation region.

does the Landau damping become very strong and the plasmon disappears as a separate excitation.

This sharp resonance peak indicates that when the acoustic plasmon first enters the $r_s=2$ single-particle excitation region the coupling to the single-particle decay channel is weak. As it penetrates deeper more decay channel states become available and the plasmon width might be expected to broaden. However, this is counteracted by the weakening of the coupling between layers as $\boldsymbol{q}$ increases. When this weakening is the dominant effect the plasmon width decreases with increasing $\boldsymbol{q}$ and this is seen in Fig. 7(b). The plasmon finally reaches the q_{c_1} threshold at which point Landau damping in the $r_s=4$ layer strongly damps the plasmon and it rapidly disappears as a distinguishable excitation. For larger layer spacings the coupling between the layers is weaker and the plasmon width is narrower. For $d=100$ nm the coupling is so weak that by the time the acoustic plasmon reaches the $r_s=2$ threshold it already resembles the $r_s=4$ plasmon so closely that its relative width never exceeds 1% for $|\boldsymbol{q}|<q_{c_1}$.

Figure 8 shows for several fixed $|\boldsymbol{q}|>q_{c_2}$ that the dynamic structure factor $S_{-}(\boldsymbol{q},\omega)\sim \mathrm{Im}\chi_{-}(\boldsymbol{q},\omega)$ is dominated by the narrow plasmon resonance right through to the $|\boldsymbol{q}|=q_{c_1}$ threshold (marked on the ω axis). The contribution to the spectral density from single-particle excitations is found to be negligible so that the plasmon saturates the spectral density. Such a sharp peak should be readily identifiable in Raman scattering measurements.

C. Electron-hole layers

In Fig. 9 we show the plasmon dispersion curves for electron-hole layers for a layer separation $d=1.05d_i$ close to the instability point. For $r_s=6.5$ this is smaller than the critical spacing d_c and there is no acoustic plasmon. Figure 9 reveals an unusual effect of correlations on the optical plasmon dispersion curve. Since correlations cause the system to relax they usually reduce the plasmon energy relative to the RPA plasmon energy. However Fig. 9 shows a case where the correlations have the opposite effect, where the optical

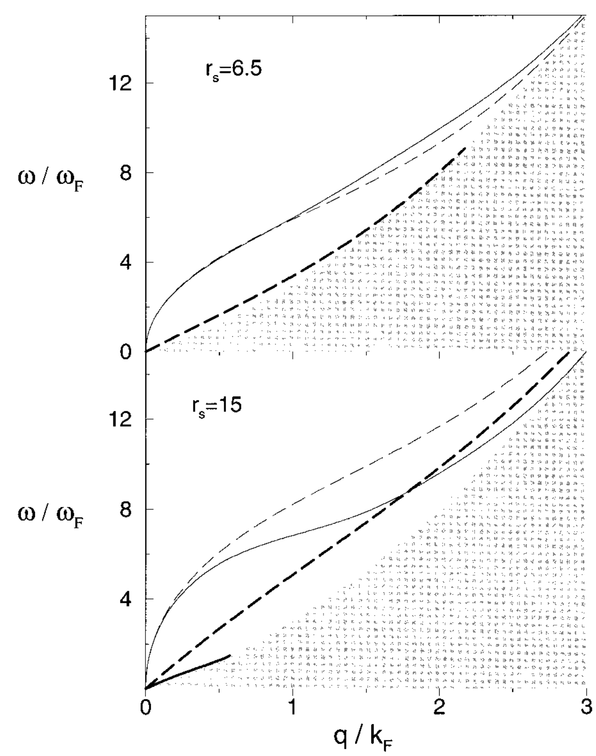

FIG. 9. Solid lines show the dispersion curves for the plasmon excitations for electron-hole layers separated by $1.05d_i$. Dashed lines are the RPA curves. Shaded area is the single-particle excitation region for a single layer at the same density.

plasmon energy is increased. This effect only occurs when attractive correlations acting between the planes dominate. This positive energy shift can most easily be understood by looking at Eq. (1) in the equal density case. There the correlations add a quantity $\{-G_{11}(\boldsymbol{q})-G_{12}(\boldsymbol{q})\exp(-|\boldsymbol{q}|d)\}V_q$ in the denominator of $\chi_-(\boldsymbol{q})$. When correlations from the attractive electron-hole interactions are sufficiently strong for the magnitude of $G_{12}(\boldsymbol{q})\exp(-|\boldsymbol{q}|d)$ to be larger than $G_{11}(\boldsymbol{q})$ then the combined net effect is to shift the plasmon energy higher. The effect occurs only near the instability and is more pronounced at higher densities where the spacing d_i is smaller. Thus for $r_s=15$ d_i is too large for the effect to occur.

VI. CONCLUSIONS

There is a notable lack of a cross dependence for the correlations acting between and within layers. An exception is near the instability for the electron-hole layer system. As expected the correlations between layers build up steadily as the layers approach each other, but at the same time except near the instability the correlations within each layer remain remarkably unaffected and continue to look like the correlations within a single layer.

Our new results for layers of unequal density are interesting because experimentally it is difficult to precisely match densities in the layers. For unequal densities we find the collective modes have qualitatively different properties from the modes for identical layers. This is because the amplitude of the plasmon oscillations is different in the two layers. The acoustic plasmon oscillations are greater in the layer of lower density and this leads to a reduction in the strength of the Landau damping when the acoustic mode first enters the single-particle excitation region. The acoustic plasmon resonance peak can be sharp until it encounters the threshold for single-particle excitations in the layer of lower density.

We have obtained a general expression for the minimum layer spacing below which the acoustic plasmon will not exist outside the single-particle excitation region and we have noted that at large wave numbers there is a crossover in behavior of the acoustic and optical plasmons from modes involving coupled oscillations in both layers to independent modes with each confined to a single layer. The wave number where this occurs depends on the layer spacing.

The strong correlations between an electron layer and a hole layer are responsible for a number of new effects. They can sometimes increase the energy of the optical plasmon. They can induce an instability in the liquid ground state to an inhomogeneous charge-density-wave ground state. They can have a marked effect on the low-lying excited-state spectrum in the form of a new soft collective mode at finite $\boldsymbol{q}$. And of course they can cause bound exciton pairs of electrons and holes to form.[16] We see evidence of a precursor of the exciton instability but it is preempted by the charge density wave instability.

ACKNOWLEDGMENTS

We thank M.P. Das, A.H. MacDonald, S. Das Sarma, G. Senatore, and J.S. Thakur for very helpful discussions. Support from the Australian Research Council and the University of New South Wales School of Physics are gratefully acknowledged.

[1] K.M. Brown, E.H. Linfield, D.A. Ritchie, G.A.C. Jones, M.P. Grimshaw, and M. Pepper, Appl. Phys. Lett. **64**, 1827 (1994).
[2] K.S. Singwi, M.P. Tosi, R.H. Land, and A. Sjölander, Phys. Rev. **176**, 589 (1968).
[3] A. Sjölander and J. Stott, Phys. Rev. B **5**, 2109 (1972).
[4] S. Das Sarma and A. Madhukar, Surf. Sci. **98**, 563 (1980).
[5] S. Das Sarma and A. Madhukar, Phys. Rev. B **23**, 805 (1981).
[6] Giuseppe E. Santoro and Gabriele Giuliani, Phys. Rev. B **37**, 937 (1988); **37**, 8443 (1988).
[7] Jainendra K. Jain and S. Das Sarma, Phys. Rev. B **36**, 5949 (1987).
[8] Adolfo Eguiluz, T.K. Lee, J.J. Quinn, and K.W. Chiu, Phys. Rev. B **11**, 4989 (1975).
[9] Narkis Tzoar and Chao Zhang, Phys. Rev. B **34**, 1050 (1986).
[10] Y. Takada, J. Phys. Soc. Jpn. **43**, 1627 (1977).
[11] G. Fasol, N. Mestres, H.P. Hughes, A. Fischer, and K. Ploog, Phys. Rev. Lett. **56**, 2517 (1986).
[12] G. Fasol, R.D. King-Smith, D. Richards, U. Ekenberg, N. Mestres, and K. Ploog, Phys. Rev. B **39**, 12 659 (1989).
[13] P.M. Platzman and P.A. Wolff, *Waves and Interactions in Solid State Plasmas* (Academic, New York, 1973), p. 103.
[14] G. Abstreiter, M. Cardona, and A. Pinczuk, in *Light Scattering in Solids IV*, edited by M. Cardona and G. Güntherodt (Springer-Verlag, Heidelberg, 1984), p. 25.
[15] L. Świerkowski, J. Szymański, and Z.W. Gortel, Phys. Rev. Lett. **74**, 3245 (1995).
[16] Yu.E. Lozovik and V.I. Yudson, Pis'ma Zh. Éksp. Teor. Fiz. **22**, 556 (1975) [JETP Lett. **22**, 274 (1975)]; Solid State Commun. **19**, 391 (1976); Fiz. Tverd. Tela (Leningrad) **18**, 1962 (1976) [Sov. Phys. Solid State **18**, 1142 (1976)]; Zh. Éksp. Teor. Fiz. **71**, 738 (1976) [Sov. Phys. JETP **44**, 389 (1976)].
[17] S.I. Shevchenko, Fiz. Nizk. Temp. **2**, 505 (1976) [Sov. J. Low Temp. Phys. **2**, 251 (1976)].
[18] A.C. Tselis and J.J. Quinn, Phys. Rev. B **29**, 3318 (1984).
[19] G. Kalman and K.I. Golden, in *Condensed Matter Theories*, edited by L. Blum and B.S. Malik (Plenum, New York, 1993), Vol. 8, p. 127.
[20] L. Świerkowski, D. Neilson, and J. Szymański, Phys. Rev. Lett. **67**, 240 (1991).
[21] B. Tanatar and D.M. Ceperley, Phys. Rev. B **39**, 5005 (1989).
[22] D. Neilson, L. Świerkowski, J. Szymański, and L. Liu, Phys. Rev. Lett. **71**, 4035 (1993).
[23] J. Szymański, L. Świerkowski, and D. Neilson, Phys. Rev. B **50**, 11 002 (1994); L. Świerkowski, D. Neilson, and J. Szymański, Aust. J. Phys. **46**, 423 (1993).
[24] A. Gold, Z. Phys. B **86**, 193 (1992).
[25] Chao Zhang, Phys. Rev. B **49**, 2939 (1994).
[26] Lian Zheng and A.H. MacDonald, Phys. Rev. B **49**, 5522 (1994).
[27] F. Stern, Phys. Rev. Lett. **18**, 546 (1967).
[28] P. Vashishta, P. Bhattacharyya, and K. S. Singwi, Nuovo Cimento **23B**, 172 (1974).